November 15, 2011

# Application of response surface methodology in optimization of photocatalytic removal of environmental pollutants using nanocatalysts

A. R. Khataee
M. B. Kasiri
L. Alidokht


Environmental Technology
Publication details, including instructions for authors and subscription information:
http://www.tandfonline.com/loi/tent20

# Application of response surface methodology in the optimization of photocatalytic removal of environmental pollutants using nanocatalysts

A. R. Khataee [a] , M. B. Kasiri [b] & L. Alidokht [a c]

[a] Department of Applied Chemistry, Faculty of Chemistry, University of Tabriz, Tabriz, Iran

[b] Faculty of Applied Arts, Tabriz Islamic Art University, Tabriz, Iran

[c] Department of Soil Science, Faculty of Agriculture, University of Tabriz, Tabriz, Iran

Available online: 15 Aug 2011

To cite this article: A. R. Khataee, M. B. Kasiri & L. Alidokht (2011): Application of response surface methodology in the optimization of photocatalytic removal of environmental pollutants using nanocatalysts, Environmental Technology, 32:15, 1669-1684

To link to this article: http://dx.doi.org/10.1080/09593330.2011.597432

*Environmental Technology*
Vol. 32, No. 15, November 2011, 1669–1684

Taylor & Francis
Taylor & Francis Group

## REVIEW ARTICLE

# Application of response surface methodology in the optimization of photocatalytic removal of environmental pollutants using nanocatalysts

A.R. Khataee[a*], M.B. Kasiri[b] and L. Alidokht[a,c]

[a]*Department of Applied Chemistry, Faculty of Chemistry, University of Tabriz, Tabriz, Iran;* [b]*Faculty of Applied Arts, Tabriz Islamic Art University, Tabriz, Iran;* [c]*Department of Soil Science, Faculty of Agriculture, University of Tabriz, Tabriz, Iran*

(*Received 17 March 2011; final version received 9 June 2011*)

Response surface methodology is a widely used technique for modelling and optimization of the photocatalytic treatment processes of water and wastewater. This methodology not only estimates linear, interaction and quadratic effects of the factors on the response, but also provides a prediction model for the response at the range of the variables studied and the optimum conditions to achieve the highest performance. The present paper reviews the results of application of this innovative methodology in modelling and optimization of the photocatalytic treatment processes. Different experimental designs including $3^k$ factorial, Doehlert, Box–Behnken and central composite designs have been developed to describe the treatment processes of dyeing effluents, pharmaceutical agents and hazardous phenolic compounds. The results showed that response surface methodology can describe the behaviour of complex reaction systems, such as photocatalytic processes, in the range of experimental conditions adopted. Optimization based on response surface methodology can also estimate the conditions of the photocatalytic processes to achieve the highest performance.

**Keywords:** photocatalyst; $TiO_2$ nanoparticles; ZnO nanoparticles; experimental design; water treatment



## Introduction

Treatment of hazardous industrial effluents is one of the growing needs of the present time. Advanced Oxidation Processes (AOPs) have been developed to convert non-biodegradable contaminants into harmless species [1–3]. Heterogeneous photocatalysis, a novel process belonging to the class of AOPs, via combination of photocatalysts, such as $TiO_2$ and ultraviolet (UV) light, is as an attractive alternative treatment method for the removal of toxic pollutants from wastewater, owing to its ability to degrade the pollutants into innocuous end-products, such as $CO_2$, $H_2$ and mineral acids [4,5]. The preferential use of $TiO_2$ for the photocatalytic degradation of organic pollutants is based on its availability, low cost and photochemical stability [6]. The photocatalytic reaction uses photons with energy greater than the band gap of a semiconductor, usually $TiO_2$, for generation of conduction band electrons and valence band holes to initiate oxidation–reduction reactions [7]. There have been several studies on the assessment of photocatalytic treatment of hazardous substances from industrial effluents [8–14].

The efficiency of a photocatalytic reaction depends on a number of factors, which govern the performance of photocatalysis. Initial concentration of pollutant, photocatalyst concentration, pH, volume of solution, radiant flux and agitation, irradiation time, light intensity, irradiation wavelength, temperature, geometrical parameters of the experimental setup and multiple degradation pathways are the parameters that can be cited. Due to the complexity and variety of influencing factors, it is difficult to evaluate the relative significance of several affecting factors, especially in the presence of complex interactions [15]. In the most recent studies, only traditional one-factor-at-a-time experiments were tested for evaluating the influence of operating factors on the photocatalytic process efficiency. This technique is not only time and work demanding, but also completely lacks representation of the effect of interaction between different factors. Response surface methodology (RSM) allows an appropriate design of the experiments, which helps to decrease the number of runs. In addition, the modelling of the system facilitates the interpretation of multivariate phenomena and is valuable tool for scaling up [16].

The purpose of RSM is to introduce statistically designed experiments to scientists who conduct the experiments for the purpose of making inferences from data. To achieve this goal, statistical considerations for preliminary planning of experiments, standard statistical designs that may be used for experiments and the underlying logic for using these designs are emphasized. It is a common but major error to view statistics as a tool to be used only after the experiments are completed. Even using their most sophisticated tools, statisticians who receive data from

*Corresponding author. Email: a_khataee@tabrizu.ac.ir; ar_khataee@yahoo.com

ISSN 0959-3330 print/ISSN 1479-487X online

http://dx.doi.org/10.1080/09593330.2011.597432
http://www.tandfonline.com

improperly designed experiments can make only vague and approximate inferences. This situation is unfortunate, because experimental data represent an expenditure of both time and money [17].

The present paper reviews the use of RSM for the optimization of photocatalytic removal of environmental pollutants using nanocatalysts. Firstly, the RSM technique and its more frequently used second-order experimental designs will be presented. Then, the removal mechanisms by nano-photocatalyst will be described. Finally, the applications of RSM experimental designs in the field of modelling and optimizing of photocatalytic removal processes will be represented.

## Response surface methodology techniques

In general, the theoretical model that relates some controllable variables to a response either is not available or is very complex. Identifying and fitting from experimental data an appropriate response surface model requires some use of statistical experimental design fundamentals, regression modelling techniques and optimization methods. As an important subject in the statistical design of experiments, RSM, introduced by Box and Wilson [18], comprises a group of mathematical and statistical techniques that is useful for empirical model building and analysis of problems in which a response of interest is influenced by several variables [19].

It is important to fit a mathematical model equation in order to approximate a relationship between response and independent variables and determine the optimum settings of these variables that result in the maximum response. Two important models are commonly used in RSM, including the first-order model (Equation (1))[20]:

$$y = \beta_0 + \sum_{i=1}^{k} \beta_i x_i + \varepsilon \quad (1)$$

and the second-order model (Equation (2)):

$$y = \beta_0 + \sum_{i=1}^{k} \beta_i x_i + \sum_{i=1}^{k} \beta_{ii} x_i^2 + \sum_{i=1}^{k} \sum_{i \neq j=1}^{k} \beta_{ij} x_i x_j + \varepsilon \quad (2)$$

where $y$ is the response, $\beta_0$ is the constant, $\beta_i$ is the slope or linear effect of the factor $x_i$, $\beta_{ii}$ is the quadratic effect of the factor $x_i$, $\beta_{ij}$ is the interaction effect between the input factors $x_i$ and $x_j$ and $\varepsilon$ is the residual term.

In most situations, the first-order models are not adequate to represent true functional relationships with independent variables, in which case a more highly structured, flexible and diversified functional second-order model should be studied in order to locate the optimum point. Adequacy of the proposed model is revealed using the diagnostic checking tests provided by analysis of variance (ANOVA).

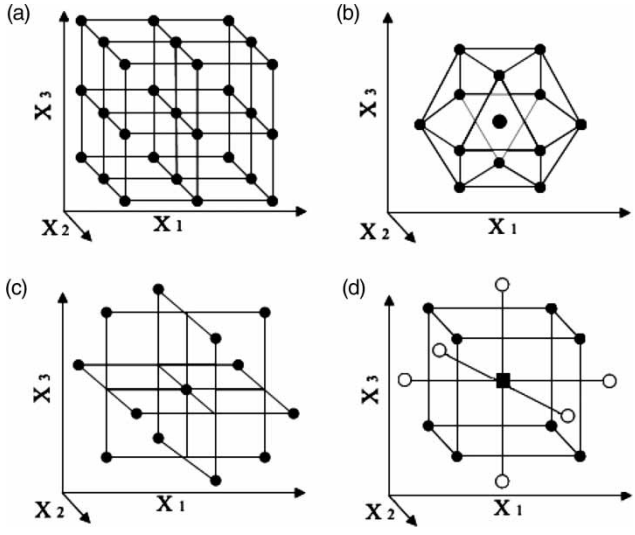


Figure 1. Experimental designs for optimization of three variables using (a) $3^k$ factorial design, (b) Doehlert design, (c) Box–Behnken design and (d) CCD ((◯) axial points, (•) factorial points and (■) central point). (Adapted from Bezerra et al. [22] with permission from the publisher, Elsevier. License Number: 2620600333602.)

### *Designs for fitting the second-order model*

The second-order model is the most-frequently used approximating polynomial model in RSM. The most common designs for the second-order model are the $3^k$ factorial, Doehlert, Box–Behnken and central composite designs (CCDs) [21,22]. These symmetrical designs differ from one another with respect to their selection of experimental points, number of levels for variables and number of runs and blocks.

#### $3^k$ *factorial design*

The $3^k$ factorial design consists of all the combinations of the levels of the control variables, which have three levels each: low, medium or centre and high [20]. The number of experimental runs ($N$) required for this design is defined as $N = 3^k$, where $k$ is the number of factors. Figure 1(a) shows the representation of the three-level factorial design for the optimization of the three variables. The $3^k$ factorial design needs a large number of experimental runs for large $k$, which causes it to lose its efficiency in the modelling of quadratic functions. Therefore, a $3^k$ factorial design will be more appropriate with factors numbering less than five. Because of its requirement for more experimental runs than can usually be accommodated in practice, designs that present a smaller number of experimental points, such as the Doehlert, Box–Behnken and CCDs, are more often used.

The application of $3^k$ factorial design is not frequent, and the use of this design has been limited to the optimization of two variables, because its efficiency is very low for a higher number of variables.

*Doehlert design*

The Doehlert (or uniform shell) design has been developed by Doehlert [23]. The Doehlert design is for heterogeneous levels of variable. This property is important when some variables are subject to restrictions, such as cost and/or instrumental constraints or when it is interesting to study a variable at major or minor levels. The intervals between each variable level present a uniform distribution [22]. The number of experiments required ($N$) for the Doehlert design is defined as $N = k^2 + k + C_0$, where $k$ is the number of factors and $C_0$ is the number of centre points. For two variables, a central point surrounded by six points from a regular hexagon represents this design. For three variables, it is represented by a geometrical solid called a cuboctahedron, and depending on how this solid is projected in the plane, it can generate some different experimental matrices. The geometry of the three-variable analogue for the Doehlert design is presented in Figure 1(b). Although its matrices are neither orthogonal nor rotatable, it presents some advantages, such as requiring few experimental points for its application and high efficiency [22,24].

Several articles can be found in the literature related to the application of the Doehlert design as a suitable tool for the optimization of hazardous substance treatment via electrochemical oxidation [25], biosorption [26], Fenton's oxidation [27,28] and the photocatalytic process [29].

*Box–Behnken design*

This design was developed by Box and Behnken [30]. The Box–Behnken design provides three levels $(-1, 0, +1)$ for each variable, which are equally spaced. The number of experiments required ($N$) is given by $N = 2k(k-1) + C_0$, where $k$ is the number of variables and $C_0$ is the number of central points. The design is represented as a cube and all points lie on a sphere of radius $\sqrt{2}$. In addition, this design does not contain any points at the vertices of the cubic region created by the upper and lower limits for each variable [31]. Figure 1(c) represents the Box–Behnken design for three-variable optimization with its 13 experimental points. This design is more economical and efficient in terms of the number of required runs than their corresponding $3^k$ designs with 27 experiments. Therefore, this design is useful in avoiding experiments that would be performed under extreme conditions, for which unsatisfactory results might occur. However, it is ineffective for situations in which we would like to know the responses at extremes.

The Box–Behnken design has been used for finding the optimum experimental conditions, leading to an optimal efficiency of different treatment processes, such as adsorption [32,33], biological treatment [34,35], Fenton's oxidation [36–38] and electrochemical [39] and photocatalytic processes [40]. However, its application in photocatalytic removal processes is still much smaller in comparison with the CCD.

*Central composite design*

The CCD presented by Box and Wilson in 1951 [18] is the design most commonly used for fitting second-order models and it has been subjected to much attention, as much in the theoretical development of its properties as in its practical use [31]. This design combines a two-level full or fractional factorial design with additional star points and at least one point at the centre of the experimental region. Figure 1(d) illustrates the CCD for the optimization of three variables. This design requires an experiment number according to $N = 2^k + 2k + C_0$, where $k$ is the number of factors and $C_0$ is the number of central points. In CCD, all factors are studied in five levels. This $N$ experiment is distributed as follows [20,31].

1. Full (or fractional) $2^k$ factorial experiments, whose factors levels are coded as $-1$, $+1$. These experiments are the only points that contribute to the estimation of the two-factor interactions.
2. Axial (or star) $2^k$ experiments with coordinates $(\pm\alpha, 0, \ldots, 0)$, $(0, \pm\alpha, \ldots, 0), \ldots, (0, 0, \ldots, \pm\alpha)$. The codified value of $\alpha$ is defined as $\alpha = (2^k)^{1/4}$. The axial points do not contribute to the estimation of interaction terms. If curvature is found in the system, the addition of axial points allows for efficient estimation of the pure quadratic terms.
3. $C_0$ central points at (0, 0,…, 0). These experiments provide an estimation of pure error and contribute to the estimation of quadratic terms.

The CCD is a rotatable and orthogonal design. A design is rotatable if the precision of the response estimation in all directions is equal and the orthogonality of the design means that different variable effects can be estimated independently.

This design has been widely used for the optimization of several treatment processes of hazardous substances, such as adsorption [41–43], Fenton's oxidation [44–51], biological treatment 52–56], electrocoagulation [57–59], reduction reactions 60,61] and photocatalytic degradation [48,62,63]. More examples for the application of CCD in photocatalytic removal processes are represented in Tables 1–3.

Other second-order designs are available, but are not as common as the ones we have already mentioned. Some of these designs include Hoke [64] designs, Box–Draper saturated designs [65] and hybrid designs [66].

## Photocatalytic removal of environmental pollutants by nanocatalysts

Photocatalytic chemistry involving semiconductor materials has grown from a subject of esoteric interest to one of central importance in both academic and technological research. In this context, environmental pollution and its control through non-toxic treatments and easy recovery

Table 1. Application of RSM in optimization of the photocatalysis of organic dyes using nanocatalysts.

| Photocatalytic process | Type and size of photocatalyst | Removal target | Selected variables | Optimization technique | Experiment number | Response function | Ref. |
|---|---|---|---|---|---|---|---|
| UV/$TiO_2$ (immobilized $TiO_2$ on non-woven paper) | $TiO_2$ Millennium PC-500, crystallites mean size 5–10 nm | C.I. Basic Blue 3 | $[Dye]_o$ (mg/l), UV light intensity ($W/m^2$), flow rate (ml/min) and reaction time (min) | CCD | 31 | Photocatalytic decolorization efficiency (%) | [98] |
| Photoelectro-Fenton combined with UV/$TiO_2$ (immobilized $TiO_2$ on non-woven paper) | $TiO_2$ Millennium PC-500, crystallites mean size 5–10 nm | C.I. Acid Red 17 | $[Fe(III)]_o$ (mM), $[Dye]_o$ (mg/l), reaction time (min) and applied current (mA) | CCD | 31 | Decolorization efficiency (%) | [99] |
| UV/$TiO_2$ (immobilized $TiO_2$ on glass plates) | $TiO_2$ Millennium PC-500, crystallites mean size 8 nm | C.I. Acid Green 25 | $[Dye]_o$ (mg/l), UV light intensity ($W/m^2$), flow rate (ml/min) and reaction time (min) | CCD | 31 | Photocatalytic decolorization efficiency (%) | [100] |
| UV/$TiO_2$ (immobilized $TiO_2$ on glass plates) | $TiO_2$ Millennium PC-500, crystallites mean size 8 nm | C.I. Acid Blue 92 and C.I. Basic Blue 3 | $[Dye]_o$ (mg/l), UV light intensity ($W/m^2$), flow rate (ml/min) and reaction time (min) | CCD | 31 | Photocatalytic decolorization efficiency (%) | [101] |
| UV/$TiO_2$ | Anatase $TiO_2$ | Reactive Red 120 | $[TiO_2]_o$ (g/l), $[Dye]_o$ (mg/l) and UV intensity ($mW/cm^2$) | CCD | 20 | Colour removal (%) and TOC[1] removal (%) | [102] |
| Solar/$TiO_2$/$H_2O_2$ ($[H_2O_2]$ = 14.7 mM, $[Dye]_o$ = 25 mg/l) | $TiO_2$ P25 Degussa | Orange II | Initial pH and $[TiO_2]_o$ (mg/l) | CCD | 11 | Pseudo-first-order kinetic rate of dye degradation ($min^{-1}$) | [103] |
| UV/$TiO_2$/$H_2O_2$ (coated $TiO_2$ on glass Raschig rings) | $TiO_2$ P25 Degussa | Orange II | Initial pH and $[H_2O_2]_o$ (mM) | CCD | 11 | Residual colour (%) after 30 min reaction | [104] |
| UV/$TiO_2$ | $TiO_2$ P25 Degussa | Reactive Metanil Yellow | $[TiO_2]_o$ (g/l), light flux (photon/s $cm^2$), $[Dye]_o$ (mg/l) and pH | CCD face-centred | 28 | Dye removal time (min) | [105] |
| UV/$TiO_2$ | $TiO_2$ P25 Degussa | Reactive Red 239 | UV light intensity ($W/m^2$), $[TiO_2]_o$ (g/l), initial pH and stirring speed (rpm) | CCD | 30 | Photocatalytic decolorization efficiency (%) | [106] |
| UV/$TiO_2$/$H_2O_2$/$Fe^{3+}$ | $TiO_2$ P25 Degussa | Reactive Black 5 | $[TiO_2]_o$ (g/l), $[Fe^{3+}]_o$ (mg/l) and $[H_2O_2]_o$ (mg/l) | CCD | 16 | Colour removal efficiency (%) after 4 min | [107] |
| UV/ZnO | ZnO, 450 nm | Congo red | $[Dye]_o$ (g/l), $[ZnO]_o$ (g/l), pH and time (h) | Box–Behnken | 29 | Photodecolorization (%) | [40] |

[1]TOC: total organic carbon.

Table 2. Application of RSM in optimization of the photocatalysis of pharmaceutical agents using nanocatalysts.

| Photocatalytic process | Type and size of photocatalyst | Removal target | Selected variables | Optimization technique | Experiment number | Response function | Ref. |
|---|---|---|---|---|---|---|---|
| UV/$TiO_2$ | $TiO_2$ P25 Degussa, size 20–30 nm | Antibiotic: oxolinic acid | Initial pH and $[TiO_2]_o$ (g/l) | $3^k$ factorial design | 11 | Photodegradation efficiency (%) after 15 min | [108] |
| UV/$TiO_2$ | Anatase $TiO_2$, size 10–20 nm | Antibiotic: chloramphenicol (CAP) | Initial pH, $[TiO_2]_o$ (g/l) and $[CAP]_o$ (mg/l) | CCD | 26 | Photodegradation efficiency (%) | [109] |
| UV/$TiO_2$ | $TiO_2$ P25 Degussa | Pharmaceutical agent: salbutamol | Initial pH and $[TiO_2]_o$ (mg/l) | CCD | 11 | Degradation efficiency (%) after 30 min | [110] |
| Vis/doped $TiO_2$ | Doped $TiO_2$ by thiourea | Antibiotic: flumequine | $[TiO_2]_o$ (g/l) and pH | CCD | 11 | Degradation efficiency (%) after 15 min | [111] |
| UV/$TiO_2$/$H_2O_2$/ $Fe^{3+}$ | $TiO_2$ P25 Degussa | Psychiatric drug: imipramine | $[TiO_2]_o$ (g/l), $[Fe^{3+}]_o$ (mg/l) and $[H_2O_2]_o$ (mg/l) | CCD | 16 | Degradation efficiency (%) after 15 min | [112] |
| UV/$TiO_2$ | $TiO_2$ P25 Degussa | Antimicrobial agent: methylparaben | pH, $[TiO_2]_o$ (g/l), $[O_2]$ (mg/l) and light intensity (photon/s $cm^2$) | CCD | 28 | Removal time of 50% methylparaben (half-time) | [113] |
| Vis/$TiO_2$/$H_2O_2$ | $TiO_2$ P25 Degussa | 4-methylbenzylidene camphor | $[TiO_2]_o$ (mg/l), $[H_2O_2]$ (mM) and light intensity ($W/m^2$) | CCD | 17 | Degradation efficiency (%) after 15 min | [114] |

Table 3. Application of RSM in optimization of the photocatalysis of phenolic compounds using nanocatalysts.

| Photocatalytic process | Type and size of photocatalyst | Removal target | Selected variables | Optimization technique | Experiment number | Response function | Ref. |
|---|---|---|---|---|---|---|---|
| UV/$TiO_2$ | $TiO_2$ P25 Degussa | Terephthalic acid | $[TiO_2]_o$ (μg/ml), [Terephthalic acid]$_o$ (mM) and time (min) | CCD | 19 | Emitted fluorescence intensity | [115] |
| UV/$TiO_2$ | Anatase $TiO_2$, (5, 10 and 32 nm) | Phenol | $TiO_2$ size (nm), $[TiO_2]_o$ (g/l), DO[1] (mg/l) and $[phenol]_o$ (mg/l) | Box–Behnken | 27 | Apparent degradation rate constant ($min^{-1}$) | [116] |
| Homogeneous photocatalysis | 2,4,6-triphenylpyrylium hydrogensulfate | Xylidine (2,4-dimethylaniline) | $[Catalyst]_o$ (mg/l) and $[Xylidine]_o$ (mg/l) | Doehlert uniform array | 10 | Degradation efficiency (%) after 15 and 60 min | [29] |
| UV/$TiO_2$ (immobilized $TiO_2$ on GAC[2]) | Anatase $TiO_2$, (7.7 nm) | Phenol | $[Phenol]_o$ (mg/l), $[H_2O_2]$ (mg/l) and photocatalyst loading (layer) | CCD | 20 | Degradation efficiency (%) after 70 min | [6] |
| UV/$TiO_2$ | $TiO_2$ P25 Degussa | Catechol | $[TiO_2]_o$ (g/l), Oxidant[3] amount (ml) and pH | CCD | 20 | Degradation efficiency (%) after 30 min | [117] |

[1]DO: dissolved oxygen.
[2]GAC: granular activated carbon.
[3]Oxidant: sodium hypochlorite containing 4% chlorine.

processes is a serious matter. The number of publications concerning mineralization of dyes, pharmaceutical agents, phenolic compounds, pesticides, fungicides, hazardous compounds, etc., has increased tremendously in the last decade [67–69].

Photocatalysis covers the range of reactions proceeding under the action of light. Among these, we find catalysis of photochemical reactions, photo-activation of catalysts and photochemical activation of catalytic processes. Photocatalysis is defined by the International Union of Pure and Applied Chemistry (IUPAC) as 'the catalytic reaction involving light absorption by a catalyst or a substrate' [70,71]. A more precise definition may be that 'photocatalysis is a change in the rate of chemical reactions or their generating under the action of light in the presence of the substances (photocatalysts) that absorb light quanta and are involved in the chemical transformations of the reaction participants, repeatedly coming with them into intermediate interactions and regenerating their chemical composition after each cycle of such interactions' [71]. The most typical processes covered by photocatalysis are the photocatalytic oxidation (PCO) and the photocatalytic decomposition (PCD) of substrates, such as organic compounds. The PCO process employs gas-phase oxygen as a direct participant to the reaction, while the PCD process takes place in the absence of molecular oxygen [70].

Several semiconductors possess band gaps that are suitable to catalyse chemical reactions. Titanium dioxide has become a 'gold standard' semiconductor in the field of photocatalysis. $TiO_2$ is chemically and biologically inert, as well as cheap to manufacture and apply. Crystals of titanium dioxide exist in three crystalline forms: rutile, anatase and brookite (Figure 2). Only anatase and rutile forms have good pigmentary properties. However, rutile is more thermally stable than anatase. Most titanium dioxide pigments, either as the rutile or the anatase form, are produced from titanium mineral concentrates through chloride or sulfate processes [72–74].

In recent years, applications of nanostructured $TiO_2$ nanomaterials in environmental pollutant remediation have been one of the most active areas in research [70,75–78]. Commercially available Degussa P25 $TiO_2$ is a highly photoactive form of $TiO_2$ composed of 20%–30% rutile and 70%–80% anatase $TiO_2$ with particle size in the range of 12–30 nm and surface area of 50 $m^2/g$. Another commercial nanostructured $TiO_2$ sample is $TiO_2$ Millennium PC-500, which is composed of 100% anatase with particle size in the range of 5–10 nm and surface area of 320 $m^2/g$. In addition to $TiO_2$ [79,80], there is a wide range of metal oxides and sulfides that have been successfully tested in photocatalytic reactions. Among these are ZnO [81], $WO_3$ [82], $WS_2$ [83], $Fe_2O_3$ [84], $V_2O_5$ [85], $CeO_2$ [86], CdS [87], coupled ZnO–$Fe_2O_3$ [88] and ZnS [89,90]. Interaction of these semiconductors with photons that possess energy equal to or higher than the band gap may cause separation of the conduction and valence bands. This event is known as electron–hole pair generation. For $TiO_2$, this energy can be supplied by photons with energy in the near UV range. This property promotes $TiO_2$ as a promising candidate in photocatalysis where solar light can be used as the energy source [70]. Some of the beneficial characteristics of nanostructured $TiO_2$ materials are high photocatalytic efficiency, physical and chemical stability, low cost and low toxicity.

When $TiO_2$ is illuminated with $\lambda < 390$ nm light, an electron excites out of its energy level and consequently leaves a hole in the valence band (Figure 3; [91]). As electrons are promoted from the valence band to the conduction band, they generate electron–hole pairs (Equation (3)) [80,92,93]:

$$TiO_2 + h\nu(\lambda < 390\ \text{nm}) \longrightarrow e^- + h^+ \qquad (3)$$

Valence band ($h^+$) potential is positive enough to generate hydroxyl radicals ($^\bullet OH$) at the $TiO_2$ surface and the conduction band ($e^-$) potential is negative enough to reduce molecular oxygen, as described in Figure 3.

The hydroxyl radical is a powerful oxidizing agent that may attack the organic matter (OM) present at or near the surface of $TiO_2$. It is capable of degrading toxic and bioresistant compounds into harmless species (e.g. $CO_2$,

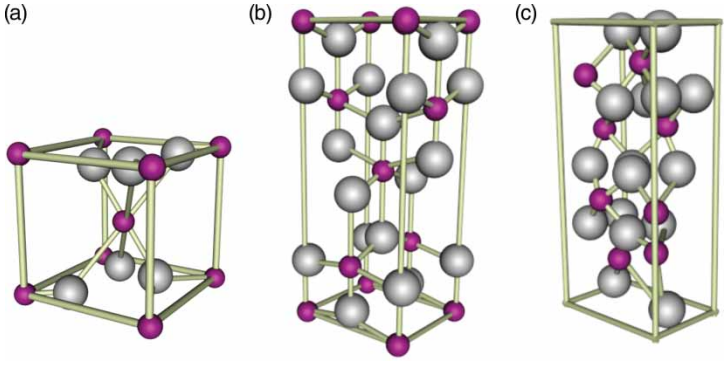


Figure 2. Unit cells of (a) rutile, (b) anatase and (c) brookite. Grey (big) and red (small) spheres represent oxygen and titanium, respectively.

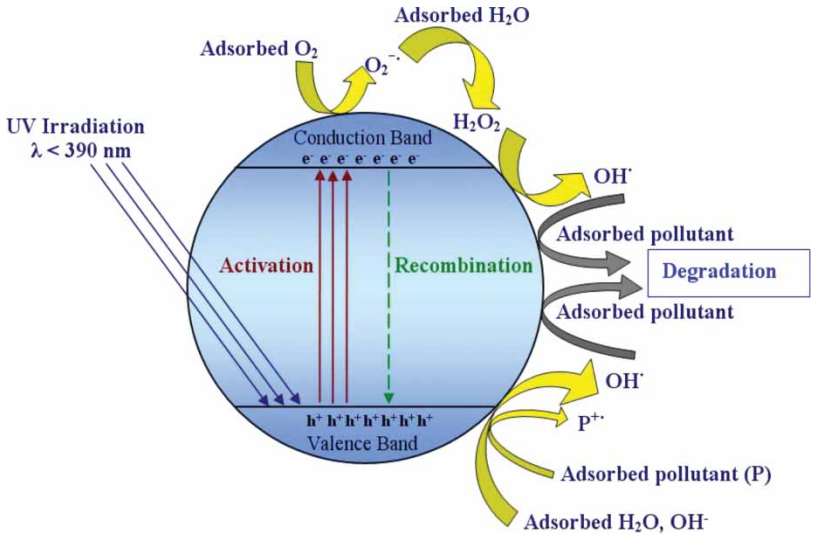


Figure 3. Photocatalytic process mechanism at the surface of $TiO_2$ nanoparticles. (Adapted from Khataee and Kasiri [91] with permission from the publisher, Elsevier. License Number: 2586970151349.)

$H_2O$, etc.). This decomposition can be explained through the following reactions [94,95]:

$$h^+_{VB} + OM \longrightarrow OM^{\bullet +} \longrightarrow \text{Oxidation of OM} \quad (4)$$

$$^{\bullet}OH_{(ads)} + OM \longrightarrow \text{Degradation of OM} \quad (5)$$

Nanostructured $TiO_2$ materials are successfully used for the photocatalytic removal of a variety of organic pollutants, such as dyes, pharmaceutical agents and phenolic hazardous compounds, as well as reduction deposition of heavy metals, such as $Pt^{4+}$, $Pd^{2+}$, $Au^{3+}$, $Rh^{3+}$ and $Cr^{3+}$ from aqueous solutions. $TiO_2$ nanomaterials have also been effective in the destruction of biological organisms, such as bacteria, viruses and moulds [96,97].

Optimization of the photocatalytic removal of organic dyes, pharmaceutical agents and phenolic compounds using nanocatalysts using RSM is summarized in Tables 1–3 [98–117].

## Optimization of photocatalytic processes using response surface methodology

In most photocatalytic processes, the theoretical model that relates some controllable variables (factors) to a response either is not available or is very complex. In conventional methods used to determine this relationship, experiments are carried out varying systematically the studied parameter and keeping the others constant. This should be repeated for all the influencing parameters, resulting in an unreliable number of experiments. In addition, this exhaustive procedure is not able to find the combined effect of the effective parameters. In this way, the information about the relation between factors and response should be obtained in an empirical way [31,41,118]. Using RSM, it is possible to estimate linear, interaction and quadratic effects of the factors and to provide a prediction model for the response.

This innovative methodology has been applied to model and optimize the photocatalytic treatment processes. Different experimental designs, including $3^k$ factorial, Doehlert, Box–Behnken and CCDs, have been used to optimize these processes [119]. Table 1 summarizes the application of RSM in the photocatalytic treatment of dyeing effluents.

Khataee et al. [98,100] and Fathinia et al. [101] have widely used RSM in photocatalytic degradation of organic dyes by a UV/$TiO_2$ process. The investigated $TiO_2$ nanoparticles were Millennium PC-500 (crystallites mean size 5–10 nm) immobilized on non-woven paper or glass plates. A CCD was developed to assess individual and interactive effects of the four main independent parameters (initial dye concentration, UV light intensity, flow rate and reaction time) on the decolorization efficiency. This design consisted of 31 experiments, including 16 experiments in cube points, 8 in axial points and 7 replications at the centre point. They have reported that predicted values of decolorization efficiency are in good agreement with experimental values ($R^2 > 0.93$). Optimization results have also proved that maximum decolorization efficiency is achieved at the optimum conditions of the variables. The time of irradiation and UV light intensity were the most important variables that influenced the efficiency of the process (Figure 4).

In another work, Khataee et al. [99] employed RSM to assess individual and interactive effects of the four main independent parameters in the photoelectron-Fenton/UV/$TiO_2$ process. The investigated nano-photocatalyst was Millennium PC-500 $TiO_2$ with crystallites of mean size of 5–10 nm immobilized on non-woven paper. A CCD with a total number of 31 experiments has been used

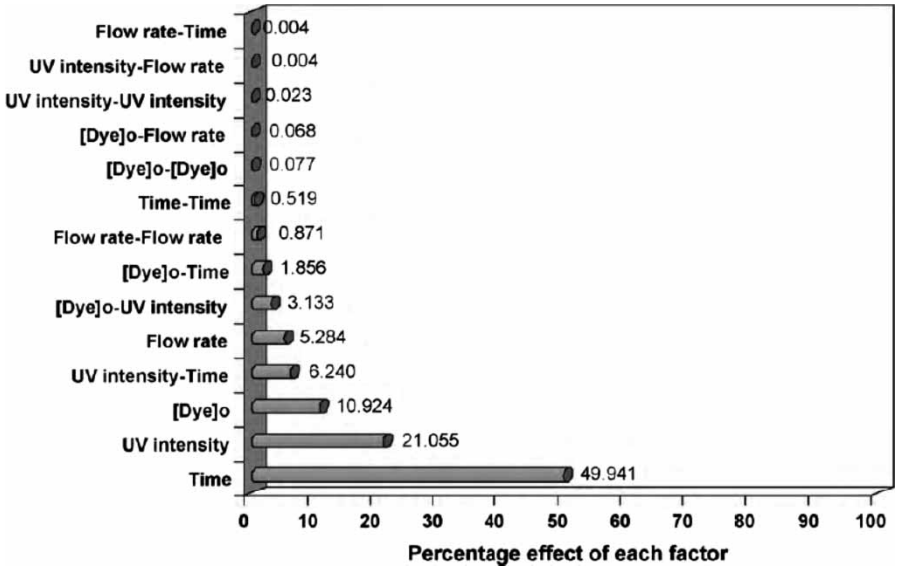


Figure 4. Pareto graphic analysis of the variables in the UV/$TiO_2$ treatment process. (Adapted from Khataee et al. [99] with permission from the publisher, Elsevier. License Number: 2603020608270.)



and, based on the ANOVA, a high determination coefficient ($R^2 = 0.978$) and satisfactory prediction second-order regression are obtained. The optimum initial amount of Fe(III), initial dye concentration, reaction time and applied current have been reported as 0.2 mM, 15 mg/l, 36 min and 100 mA, respectively. The results showed that RSM is a suitable method to optimize the operating conditions. Graphical response surface and contour plots were also used to locate the optimum point.

Degradation of azo dye Reactive Red 120 in a UV/$TiO_2$ process has been optimized by Cho and Zoh [102] using a RSM based on the CCD. The effect of three main parameters, including the amount of $TiO_2$ nanoparticles, dye concentration and UV light intensity, has been investigated on the response variables, including colour removal and the solution total organic carbon (TOC) abatement. These experiments have been carried out as a CCD consisting of 20 experiments determined by the $2^3$ full-factorial designs with six axial points and six centre points. The degradation of the azo dye followed an apparent first-order rate law in every pH condition. The report showed that the responses of colour removal in photocatalysis of dyes were significantly affected by the synergistic effect of the linear term of UV intensity and the antagonistic effect of the quadratic term of UV intensity. Significant factors and synergistic effects for the TOC removal were the linear terms of $TiO_2$ and UV intensity.

Monteagudo and Durán [103] studied the application of RSM in the decolorization and mineralization process of azo dye Orange II under artificial UV light and solar energy concentrated by a Fresnel lens in the presence of hydrogen peroxide and $TiO_2$-P25. In total, 11 experiments have been done in a CCD and this methodology allows the authors to fit the optimal values of the parameters: pH and catalyst concentration leading to the total solar degradation of orange II. The response surface modelling in a three-dimensional plot for pH, $TiO_2$ nanoparticle concentration and the kinetic rate constant of the decolorization reaction were also presented in this work.

Moreover, RSM has been used for modelling of the decolorization and mineralization of azo dye Orange II in a photoreactor using $TiO_2$-coated glass rings as the immobilized photocatalyst [104]. In this work, Fernández et al. carried out a total of 11 experiments in a factorial design to predict the optimal values of the parameters leading to Orange II abatement. The photocatalytic degradation of Orange II was followed by spectrophotometric analysis and TOC measurements. The authors proposed a single mathematical expression obtained from modelling of the experimental results that is successfully able to predict the value of the response as a function of influencing variables, including the solution pH and concentration of $H_2O_2$.

Sleiman et al. [105] developed an experimental design based on RSM. This design was applied to assess the individual and interaction effects of several operating parameters (dye concentration, $TiO_2$ concentration, pH, light flux, etc.) on the treatment efficiency of Metanil Yellow in aqueous solution using $TiO_2$ nanoparticles as the photocatalyst under UV irradiation. In total, 28 experiments were carried out in a CCD face-centred design and, based on the experimental design data, a semi-empirical expression was obtained, permitting one to predict and optimize the dye removal time. The authors showed that the results are very consistent with experiment values ($R^2 = 0.995$). Additional experiments have been done under near-optimal conditions

where the results obtained are found to be very close to the predicted values.

In another work, RSM has been applied to optimize four independent parameters, including UV light intensity, the concentration of $TiO_2$, initial pH and stirring speed, in the photocatalytic degradation process of the dye Reactive Red 239 [106]. Titanium dioxide powder Degussa P25 with greater than 99.5% purity (average primary particle size: 21 nm, Brunauer–Emmett–Teller (BET) surface area: $50 \pm 15\ m^2/g$) was used in this study. To obtain the mutual interaction between these four parameters and to optimize these parameters during the process, Liu and Chiou applied the results of 30 experiments in a $2^4$ full-factorial CCD. The results obtained indicate that the concentration of $TiO_2$ has a significant positive effect on the efficiency of decolorization. They have reported the optimized condition of the photocatalytic degradation of the dye as $16.08\ W/m^2$ UV light intensity, 3.06 g/l $TiO_2$ concentration, 2.64 initial pH and 880 rpm stirring speed. Under this condition, the maximal decolorization efficiency of 99.82% was achieved.

In another work by Secula et al. [107], RSM has been applied for modelling and optimization of the photocatalytic decolorization of a simulated dyestuff effluent, containing the azo dye Reactive Black 5 (RB5). They chose the initial concentration of $TiO_2$ nanoparticles (P25), $Fe^{3+}$ and $H_2O_2$ as influencing variables in a CCD and in total 16 experiments were carried out. The multivariate experimental design allowed the development of a quadratic model as a functional relationship between colour removal efficiency and the independent variables. The authors have reported that under the optimum conditions established, the performance of 99.3% for colour removal was experimentally reached. It was found that all factors considered had an important effect in the decolorization efficiency of the OM abatement.

The Box–Behnken design was also employed by Annadurai et al. [40] to study the effect of different variables on the photocatalytic decolorization of Congo red under sunlight illumination using ZnO catalyst. Four variables, including the dye concentration, weight of catalyst ZnO, pH and reaction time, have been chosen to identify the significant effects and interactions in the batch studies. According to the design selected, 29 experiments have been carried out and a second-order polynomial regression model has been developed using the experimental results. They have found that the photodecolorization potential of ZnO is strongly affected by the variations in the dye concentration, weight of catalyst ZnO, pH and reaction time. The experimental values were in good agreement with the predicted values and the $R^2$ value was found to be 0.9982. The maximum percentage of photodecolorization of 97% has been achieved in optimum conditions of the variables, including the dye concentration of 0.05 g/l, ZnO 0.16 g/l, pH 7.0 and reaction time of 2.0 h.

RSM has also been widely used in the photocatalytic removal of pharmaceutical agents and Table 2 summarizes the results of these works. For instance, in an interesting work, response methodology and the Pareto diagram have been used to evaluate the effects of catalyst load (0.2–1.5 g/l) and pH (7.5–11) on the degradation of 20 mg/l of antibiotic oxolinic acid in a photocatalytic system using $TiO_2$ Degussa P-25 in suspension [108]. A $3^k$ factorial design was developed and in total 11 experiments were carried out. Under optimal conditions the evolution of the substrate, chemical oxygen demand (COD), dissolved organic carbon, toxicity and antimicrobial activity on *Escherichia coli* cultures were evaluated. The authors indicated that, under optimal conditions, pH 7.5 and 1.0 g/l of $TiO_2$ and after 30 min, the $TiO_2$ photocatalytic system was able to eliminate both the substrate and the antimicrobial activity, and to reduce the toxicity of the solution by 60%. Figure 5 illustrates the obtained response surface diagram for oxolinic degradation percentage.

The experimental design methodology, including a CCD, has been also applied for modelling and optimization of the operational parameters on photocatalytic degradation of chloramphenicol (CAP) using $TiO_2$ nanoparticles [109]. The multivariate experimental design was employed to establish a quadratic model as a functional relationship between the degradation rate of CAP and three experimental parameters, including pH, $TiO_2$ concentration and CAP initial concentration. The results of 26 experiments were analysed to obtain the interaction effects and optimal value of parameters. The authors reported that the optimal values of the operational parameters under the related constraint conditions are pH 6.4, $TiO_2$ concentration of 0.94 g/l and CAP initial concentration of 19.97 mg/l. Under these conditions, the degradation rate of CAP approached 85.97%. The $R^2$ value (0.9519) proved a good agreement between the experimental results and the predictive values. Application

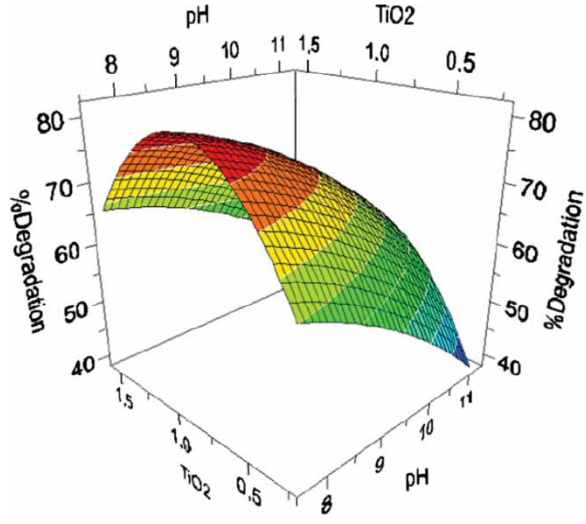


Figure 5. Optimization of $TiO_2$ load and pH for the photocatalytic degradation of oxolinic acid (20 mg/l) using a response surface diagram. (Adapted from Giraldo et al. [108] with permission from the publisher, Elsevier. License Number: 2620591491435.)

of RSM in this work revealed that pH and $TiO_2$ concentrations have a significant influence on the degradation rate of CAP.

Sakkas et al. [110] applied the CCD to investigate the simultaneous effect of $TiO_2$ concentration and pH and the interactions between these two variables in the photocatalytic degradation of pharmaceutical agent salbutamol. In a CCD, 11 experiments were performed, at which the two variables ($TiO_2$ concentration and pH) were codified in five levels with three central points for statistical validity. The equations used to quantitatively describe each system and draw the response surface were built based on the experimental data obtained for salbutamol degradation (%) after 30 min of irradiation during the photocatalytic treatment procedure. Predicted salbutamol degradation (%) was in good agreement with the observed values (Figure 6). RSM allowed fitting of the optimal values of the parameters leading to the degradation of the micropollutant.

RSM was used to describe the degradation process of antibiotic flumequine with synthesized doped-$TiO_2$ under solar-simulated irradiation [111]. The doping agent of $TiO_2$ samples was urea or thiourea. The RSM model was based on a central composite circumscribed design made of a factorial design and star points. The selected variables were $TiO_2$ nanoparticle amounts and pH, while the response factor was flumequine degradation after 15 min of irradiation. According to this design, 11 experiments were carried out and a second-order function that described the system behaviour was proposed by a multiple regression. The statistical validation was performed by an ANOVA test with a 95% of confidence. The authors reported that an excellent correspondence between experimental and calculated values presents an average variation coefficient of less than 2%, validating the polynomial.

Calza et al. [112] also developed a multivariate experimental design to optimize the catalytic degradation of imipramine solutions under simulated solar irradiation. Experiments were carried out using $TiO_2$ Degussa P25 as the photocatalyst. In this work, CCD was applied to analyse the simultaneous effect of $H_2O_2$, Fe(II) and $TiO_2$ in the photocatalytic degradation process, as well as to evaluate the interactions between the studied variables. This design considered low (−) and high (+) levels, as well as central points (0) for the $H_2O_2$, Fe(II) and $TiO_2$ concentrations. In total, 16 experiments were carried out and, based on the results of CCD, the authors found that $TiO_2$ is the most significant factor affecting imipramine degradation, followed by $H_2O_2$ and Fe(II).

As an another example of RSM application in photocatalytic processes, multivariable CCD has been applied for modelling of photocatalytic degradation of bactericide methylparaben [113]. This methodology was used to estimate the individual and interaction factors, including pH, $TiO_2$ loading, oxygen concentration and light flux. After carrying out 28 experiments according to the design selected, a semi-empirical expression with high $R^2$ value (0.9896) was obtained via data analysis to predict the response of 50% methylparaben removal time. In addition, an optimal experimental region was obtained through the contour diagram plots in this work. The authors reported the optimal experimental conditions as an achievement

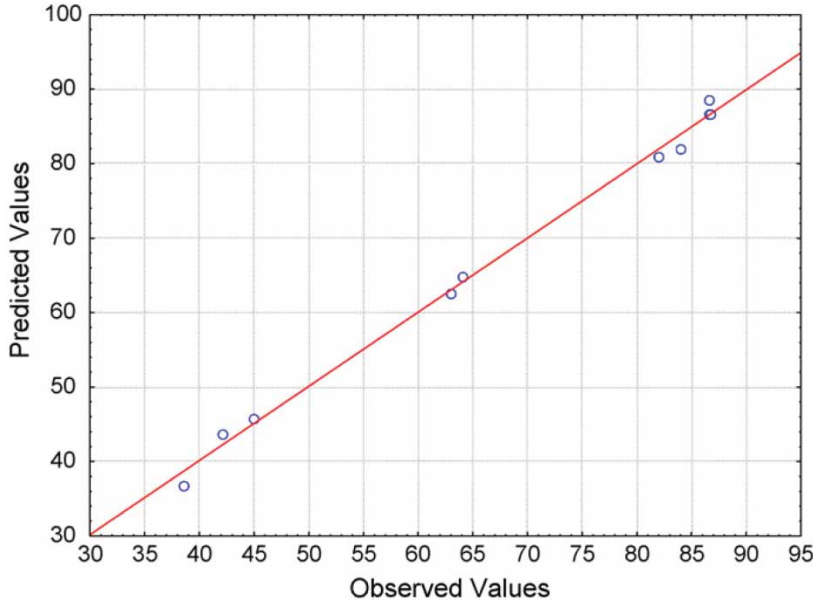


Figure 6. Comparison of predicted values of degradation with experimental values. (Adapted from Sakkas et al. [110] with permission from the publisher, Elsevier. License Number: 2603021296340.)

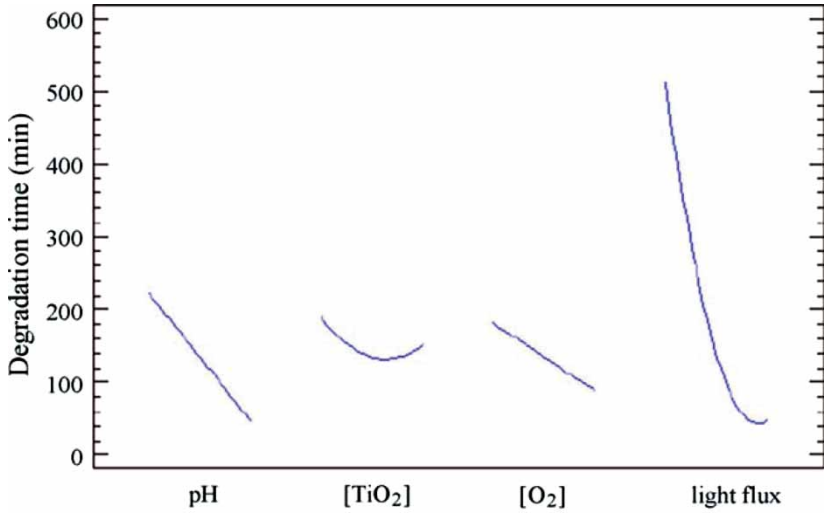


Figure 7. Graphical presentation of the statistical evaluation of the effects of individual factors on the methylparaben photocatalysis. (Adapted from Lin et al. [113] with permission from the publisher, Elsevier. License Number: 2603030441081.)



of experimental design (pH 9, $TiO_2$ loading 2.5 g/l, dissolved oxygen (DO) concentration 18 mg/l and light flux $5.8 \times 10^{15}$ photons $s^{-1}$ $cm^{-2}$). The authors have shown that there are two photocatalytic degradation regimes with respect to the UV light flux in the range studied: (i) at low light intensities, the half-life decreases linearly with increasing light intensity (first order), which means the photons are converted into active species to take part in the photocatalytic degradation immediately; and (ii) at intermediate light intensities beyond a certain value, the rate varied as functional order between zero and one (Figure 7).

In a similar work of $TiO_2/H_2O_2$ process optimization, Sakkas et al. [114] developed a CCD in combination with 'profiling and desirability function' to evaluate the effects of the main variables ($TiO_2$, $H_2O_2$ and light intensity) on 4-methylbenzylidene camphor photocatalytic degradation. In this study, the desirability function was used to identify optimum degradation efficiency (%) by calculating specific factor optimizations simultaneously. By using CCD with the desirability function, the authors reported that 80.92% degradation of 4-MBC is possible within the studied parameter levels.

RSM has been also used in modelling of the photocatalytic removal of phenolic compounds (Table 3). Eremia et al. [115] also optimized the formation of hydroxyl radicals (°OH) by $TiO_2$ nano-photocatalyst using the RSM technique. The combination of irradiation time, $TiO_2$ concentration and terephthalic acid concentration was varied at designed points of a central composite rotatable design. Following 19 experiments carried out according to a CCD, the authors reported that the three factors chosen have a significant effect upon the reaction rate. The optimum conditions for the reaction achievement were estimated to be 10 min for the irradiation time, 25 μg/ml $TiO_2$ and 0.1 mmol/l terephthalic acid concentrations. Out of three main factors and three potential interactions researched, it was found that the irradiation time, $TiO_2$ concentration, terephthalic acid concentration, irradiation time × terephthalic acid concentration and $TiO_2$ concentration × terephthalic acid concentration are the factors and the interactions that significantly affect the fluorescence process. Good agreement has been observed between the values predicted by the experimental design and the values obtained experimentally ($R^2 = 0.9280$).

Mansilla et al. [63] studied the photocatalytic degradation of ethylene diamine tetra acetic acid (EDTA), which is widely used in pharmaceutical and agricultural fields, solutions (5 mM) under different conditions in the presence of $TiO_2$ in suspension and in the presence of Fe(III). Using the CCD, the initial pH, amount of photocatalyst and the Fe/EDTA molar ratio were optimized in order to obtain maximum degradation. They found that under optimized conditions, 90% EDTA degradation (at a 0.28 Fe/EDTA molar ratio) can be reached after 60 min illumination at pH 3.0 and using 0.73 g/l $TiO_2$.

The photocatalytic degradation of hydroxyl butanedioic acid in a single $TiO_2$-coated fibre-optic reactor was investigated by Danion et al. [62] by the means of experimental design. The photocatalytic activity was mathematically described as a function of $TiO_2$ film thickness and coating length and was optimized using CCD. The optimal degradation of hydroxyl butanedioic acid for the 1 mm fibre for 15 layers and a coating length of 12.5 cm was 46%, and for the 0.6 mm fibre the optimal degradation for nine layers and a coating length of 13.5 cm was 32%. The results obtained from this study reveal that CCD is a suitable method to optimize the operating conditions of photocatalytic degradation of hydroxyl butanedioic acid.

Martins et al. [48] maximized the degradation of Amoxicillin (a pharmaceutical) via a heterogeneous photocatalytic process (HPP) and a photo-Fenton process (PFP), using the CCD method. The chosen variables were pH, $TiO_2$ concentration (mg/l) and temperature (°C) for the HPP, and pH, $H_2O_2$ concentration (mg/l) and $Fe^{2+}$ concentration (mg/l) for the PFP. The maximal degradation efficiency (COD reduction) (44.0%) using the HPP was achieved at 800 mg/l of $TiO_2$, pH = 3, 30°C and 60 min of the reaction. The best result from the optimization of the PFP (64.6% COD reduction) was obtained using pH = 3, 528 mg/l of $H_2O_2$, 255 mg/l of $Fe^{2+}$ and 60 min of the reaction. The authors claimed that the higher COD reduction obtained by the PFP does not necessarily mean that, when compared to the HPP, this process was the most suitable. They also showed that when the degradation of the amoxicillin in this effluent was carried out by means of the PFP, a photodegradation of 85% was obtained in 60 min, while by means of the HPP, a total photodegradation occurred in only 30 min of treatment.

In an interesting modelling study, a four-factor three-level Box–Behnken design has been developed by Ray et al. [116] to describe the photocatalytic degradation of phenol in an aqueous media. They selected four process variables, including $TiO_2$ catalyst size (i.e. 5, 10 and 32 nm), $TiO_2$ concentration, DO concentration and phenol concentration. In total, 27 experiments were carried out in a Box–Behnken design and, based on the results obtained, the authors have reported that a response outcome computed using experimental data for the 10 nm nanoparticle size catalyst is 13% less than the maximum value. The model successfully predicted a maximum degradation rate (0.083 $min^{-1}$) with conditions set at 9.091 nm $TiO_2$ particle size, 1.0 g/l $TiO_2$, 31.0 mg/l DO and 40 mg/l phenol.

The influence of the photocatalyst (Y-zeolites containing the 2,4,6-triphenylpyrylium cation) and substrate concentrations on xylidine oxidation by catalytic process has been investigated in another work of experimental design methodology by Amat et al. [29]. A series of experiments were chosen according to the Doehlert uniform array and a total of 10 experiments were carried out. The empirical models and the corresponding response surfaces obtained from data analysis were used successfully for simulating and predicting the degradation efficiency.

From the above studies, it can be concluded that RSM can describe the behaviour of the complex reaction system, such as photocatalytic processes in the range of experimental conditions adopted. Optimization based on RSM can estimate the conditions of the photocatalytic processes in order to achieve the highest performance.

## Conclusions

RSM is a useful and powerful tool for the estimation of linear, interaction and quadratic effects of the factors on the response. This methodology provides a prediction model for the response for the range of variables studied and the optimum conditions in order to achieve the highest performance. The results of this review show that different experimental designs, including $3^k$ factorial, Doehlert, Box–Behnken and CCDs, have been successfully developed to optimize the photocatalytic treatment processes of dyeing effluents, pharmaceutical agents and hazardous phenolic compounds. CCD is one of the most frequently used ones for the optimization of such photocatalytic treatment processes, which leads to a strong estimation of the optimum response. In almost all of the papers, the high value of the determination coefficient between the values predicted by the empirical model and the values obtained experimentally, proved the success of RSM in the modelling and optimization of the process.

## Acknowledgement

The authors thank the University of Tabriz and Tabriz Islamic Art University for financial and other support.

## References

[1] C. Galindo, P. Jacques, and A. Kalt, *Photooxidation of the phenylazonaphthol AO20 on $TIO_2$: kinetic and mechanistic investigations*, Chemosphere 45 (2001), pp. 997–1005.

[2] N. Daneshvar and A.R. Khataee, *Removal of Azo Dye C.I. Acid Red 14 from contaminated water using Fenton, $UV/H_2O_2$,$UV/H_2O_2/Fe(II)$, $UV/H_2O_2/Fe(III)$ and $UV/H_2O_2/Fe(III)$/oxalate processes: a comparative study*, J. Environ. Sci. Health, Part A 41 (2006), pp. 315–328.

[3] N. Daneshvar, D. Salari, A. Niaei, and A.R. Khataee, *Photocatalytic degradation of the herbicide erioglaucine in the presence of nanosized titanium dioxide: comparison and modeling of reaction kinetics*, J. Envniron. Sci. Health, Part B 41 (2006), pp. 1273–1290.

[4] A.R. Khataee, H. Aleboyeh, and A. Aleboyeh, *Crystallite phase-controlled preparation, characterisation and photocatalytic properties of titanium dioxide nanoparticles*, J. Exp. Nanosci. 4 (2009), pp. 121–137.

[5] A.R. Khataee, V. Vatanpour, and A.R. Amani Ghadim, *Decolorization of C.I. Acid Blue 9 solution by UV/Nano-$TiO_2$, Fenton, Fenton-like, electro-Fenton and electrocoagulation processes: a comparative study*, J. Hazard. Mater. 161 (2009), pp. 1225–1233.

[6] J.-C. Sin, S.-M. Lam, and A. Mohamed, *Optimizing photocatalytic degradation of phenol by $TiO_2$/GAC using response surface methodology*, Korean J. Chem. Eng. 28 (2011), pp. 84–92.

[7] D. Vildozo, C. Ferronato, M. Sleiman, and J.-M. Chovelon, *Photocatalytic treatment of indoor air: Optimization of 2-propanol removal using a response surface methodology (RSM)*, Appl. Catal., B 94 (2010), pp. 303–310.

[8] M. Karkmaz, E. Puzenat, C. Guillard, and J.M. Herrmann, *Photocatalytic degradation of the alimentary azo dye amaranth: mineralization of the azo group to nitrogen*, Appl. Catal., B 51 (2004), pp. 183–194.

[9] A.R. Khataee, M.N. Pons, and O. Zahraa, *Photocatalytic degradation of three azo dyes using immobilized $TiO_2$ nanoparticles on glass plates activated by UV light irradiation: influence of dye molecular structure*, J. Hazard. Mater. 168 (2009), pp. 451–457.

[10] A.R. Khataee, *Photocatalytic removal of C.I. Basic Red 46 on immobilized $TiO_2$ nanoparticles: Artificial neural network modelling*, Environ. Technol. 30 (2009), pp. 1155–1168.

[11] M.C. Yeber, C. Soto, R. Riveros, J. Navarrete, and G. Vidal, *Optimization by factorial design of copper (II) and toxicity removal using a photocatalytic process with $TiO_2$ as semiconductor*, Chem. Eng. J. 152 (2009), pp. 14–19.

[12] S.-y. Ye, Q.-m. Tian, X.-l. Song, and S.-c. Luo, *Photoelectrocatalytic degradation of ethylene by a combination of $TiO_2$ and activated carbon felts*, J. Photochem. Photobiol., A 208 (2009), pp. 27–35.

[13] S. Mozia, M. Tomaszewska, and A.W. Morawski, *Photocatalytic degradation of azo-dye Acid Red 18*, Desalination 185 (2005), pp. 449–456.

[14] C. Lizama, C. Bravo, C. Caneo, and M. Ollino, *Photocatalytic degradation of surfactants with Immobilized $TiO_2$: comparing two reaction systems* Environ. Technol. 26 (2005), pp. 909–914.

[15] N. Barka, M. Abdennouri, A. Boussaoud, A. Galadi, M. Baâlala, M. Bensitel, A. Sahibed-Dine, K. Nohair, and M. Sadiq, *Full factorial experimental design applied to oxalic acid photocatalytic degradation in $TiO_2$ aqueous suspension*, Arab. J. Chem. (2011) DOI: 10.1016/j.arabic.2010.12.015

[16] A.M. Braun, L. Jakob, E. Oliveros, and C.A.O. do Nascimento, *Up-Scaling Photochemical Reactions*, John Wiley & Sons, Inc., Hoboken, New Jersey, USA 2007, pp. 235–313.

[17] D.M. Wardrop and R.H. Myers, *Some response surface designs for finding optimal conditions*, J. Stat. Plann. Infer. 25 (1990), pp. 7–28.

[18] G.E.P. Box and K.B. Wilson, *On the experimental attainment of optimum conditions*, J. Roy. Stat. Soc. B Stat. Meth. 13 (1951), pp. 1–14.

[19] D.C. Montgomery, *Design and Analysis of Experiments: Response Surface Method and Designs*, John Wiley and Sons, Inc, New York, 2005.

[20] A.I. Khuri and S. Mukhopadhyay, *Response surface methodology*, Wiley Interdiscip. Rev. Comput. Stat. 2 (2010), pp. 128–149.

[21] V.A. Sakkas, M. Azharul Islam, C. Stalikas, and T.A. Albanis, *Photocatalytic degradation using design of experiments: a review and example of the Congo red degradation*, J. Hazard. Mater. 175 (2010), pp. 33–44.

[22] M.A. Bezerra, R.E. Santelli, E.P. Oliveira, L.S. Villar, and L.A. Escaleira, *Response surface methodology (RSM) as a tool for optimization in analytical chemistry*, Talanta 76 (2008), pp. 965–977.

[23] D.H. Doehlert, *Uniform shell designs*, J. Roy. Stat. Soc. C Appl. Stat. 19 (1970), pp. 231–239.

[24] C.R.T. Tarley, G. Silveira, W.N.L. dos Santos, G.D. Matos, E.G.P. da Silva, M.A. Bezerra, M. Miró, and S.L.C. Ferreira, *Chemometric tools in electroanalytical chemistry: methods for optimization based on factorial design and response surface methodology*, Microchem. J. 92 (2009), pp. 58–67.

[25] S. Hammami, A. Ouejhani, N. Bellakhal, and M. Dachraoui, *Application of Doehlert matrix to determine the optimal conditions of electrochemical treatment of tannery effluents*, J. Hazard. Mater. 163 (2009), pp. 251–258.

[26] J. Zolgharnein, A. Shahmoradi, and M.R. Sangi, *Optimization of Pb(II) biosorption by Robinia tree leaves using statistical design of experiments*, Talanta 76 (2008), pp. 528–532.

[27] S. Hammami, N. Oturan, N. Bellakhal, M. Dachraoui, and M.A. Oturan, *Oxidative degradation of direct orange 61 by electro-Fenton process using a carbon felt electrode: application of the experimental design methodology*, J. Electroanal. Chem. 610 (2007), pp. 75–84.

[28] A.K. Abdessalem, N. Oturan, N. Bellakhal, M. Dachraoui, and M.A. Oturan, *Experimental design methodology applied to electro-Fenton treatment for degradation of herbicide chlortoluron*, Appl. Catal., B 78 (2008), pp. 334–341.

[29] A.M. Amat, A. Arques, S.H. Bossmann, A.M. Braun, S. Göb, M.A. Miranda, and E. Oliveros, *Oxidative degradation of 2,4-xylidine by photosensitization with 2,4,6-triphenylpyrylium: homogeneous and heterogeneous catalysis*, Chemosphere 57 (2004), pp. 1123–1130.

[30] G.E.P. Box and D.W. Behnken, *Some new three-level designs for the study of quantitative variables*, Technometrics 2 (1960), pp. 455–475.

[31] S. Brown, R. Tauler, and R. Walczak, *Comprehensive Chemometrics*, Vol. 1, Elsevier, Amsterdam 2009, pp. 345–390.

[32] J. Goel, K. Kadirvelu, C. Rajagopal, and V.K. Garg, *Removal of lead(II) from aqueous solution by adsorption on carbon aerogel using a response surface methodological approach*, Ind. Eng. Chem. Res. 44 (2005), pp. 1987–1994.

[33] N. Kannan, A. Rajakumar, and G. Rengasamy, *Optimisation of process parameters for adsorption of metal ions on straw carbon by using response surface methodology*, Environ. Technol. 25 (2004), pp. 513–522.

[34] M.Y. Pamukoglu and F. Kargi, *Removal of Cu(II) ions by biosorption onto powdered waste sludge (PWS) prior to biological treatment in an activated sludge unit: a statistical design approach*, Bioresour. Technol. 100 (2009), pp. 2348–2354.

[35] R.O. Cristovao, A.P.M. Tavares, J.M. Loureiro, R.A.R. Boaventura, and E.A. Macedo, *Optimization of reactive dye degradation by Laccase using Box-Behnken design*, Environ. Technol. 29 (2008), pp. 1357–1364.

[36] E. Pollution, F. Ay, E.C. Catalkaya, and F. Kargi, *Advanced oxidation of Direct Red (DR 28) by Fenton treatment*, Environ. Eng. Sci. 25 (2008), pp. 1455–1462.

[37] I. Grcic, D. Vujevic, J. Sepcic, and N. Koprivanac, *Minimization of organic content in simulated industrial wastewater by Fenton type processes: a case study*, J. Hazard. Mater. 170 (2009), pp. 954–961.

[38] M. Dopar, H. Kusic, and N. Koprivanac, *Treatment of simulated industrial wastewater by photo-Fenton process. Part I: the optimization of process parameters using design of experiments (DOE)*, Chem. Eng. J. (2010), DOI:10.1016/j.ce.j.2010.09.070

[39] M. Li, C. Feng, Z. Zhang, R. Chen, Q. Xue, C. Gao, and N. Sugiura, *Optimization of process parameters for electrochemical nitrate removal using Box-Behnken design*, Electrochim. Acta 56 (2010), pp. 265–270.

[40] G. Annadurai, T. Sivakumar, and S. Rajesh Babu, *Photocatalytic decolorization of congo red over ZnO powder using Box-Behnken design of experiments*, Bioprocess Biosyst. Eng. 23 (2000), pp. 167–173.

[41] S.C.R. Santos and R.A.R. Boaventura, *Adsorption modelling of textile dyes by sepiolite*, Appl. Clay Sci. 42 (2008), pp. 137–145.

[42] S. Aber, A. Khataee, and M. Sheydaei, *Optimization of activated carbon fiber preparation from Kenaf using $K_2HPO_4$ as chemical activator for adsorption of phenolic compounds*, Bioresour. Technol. 100 (2009), pp. 6586–6591.

[43] F. Oughlis-Hammache, N. Hamaidi-Maouche, F. Aissani-Benissad, and S. Bourouina-Bacha, *Central composite*

*design for the modeling of the phenol adsorption process in a Fixed-Bed reactor*, J. Chem. Eng. Data 55 (2010), pp. 2489–2494.

[44] M. Ahmadi, F. Vahabzadeh, B. Bonakdarpour, E. Mofarrah, and M. Mehranian, *Application of the central composite design and response surface methodology to the advanced treatment of olive oil processing wastewater using Fenton's peroxidation*, J. Hazard. Mater. 123 (2005), pp. 187–195.

[45] E.C. Catalkaya and F. Kargi, *Effects of operating parameters on advanced oxidation of diuron by the Fenton's reagent: a statistical design approach*, Chemosphere 69 (2007), pp. 485–492.

[46] M.B. Kasiri, H. Aleboyeh, and A. Aleboyeh, *Modeling and optimization of heterogeneous photo-Fenton process with response surface methodology and artificial neural networks*, Environ. Sci. Technol. 42 (2008), pp. 7970–7975.

[47] C.S.D. Rodrigues, L.M. Madeira, and R.A.R. Boaventura, *Optimization of the azo dye Procion Red H-EXL degradation by Fenton's reagent using experimental design*, J. Hazard. Mater. 164 (2009), pp. 987–994.

[48] A.F. Martins, F. Mayer, E.C. Confortin, and C.d.S. Frank, *A study of photocatalytic processes involving the degradation of the organic load and Amoxicillin in hospital wastewater*, CLEAN - Soil Air Water 37 (2009), pp. 365–371.

[49] A.R. Khataee, M. Zarei, and L. Moradkhannejhad, *Application of response surface methodology for optimization of azo dye removal by oxalate catalyzed photoelectro-Fenton process using carbon nanotube-PTFE cathode*, Desalination 258 (2010), pp. 112–119.

[50] V. Homem, A. Alves, and L. Santos, *Amoxicillin degradation at ppb levels by Fenton's oxidation using design of experiments*, Sci. Total Environ. 408 (2010), pp. 6272–6280.

[51] A. Aris and P.N. Sharratt, *Influence of initial dissolved oxygen concentration on Fenton's reagent degradation*, Environ. Technol. 27 (2006), pp. 1153–1161.

[52] D. Ranjan, P. Srivastava, M. Talat, and S. Hasan, *Biosorption of Cr(VI) from water using biomass of Aeromonas hydrophila: central composite design for optimization of process variables*, Appl. Biochem. Biotech. 158 (2009), pp. 524–539.

[53] B. Kiran, A. Kaushik, and C.P. Kaushik, *Response surface methodological approach for optimizing removal of Cr (VI) from aqueous solution using immobilized cyanobacterium*, Chem. Eng. J. 126 (2007), pp. 147–153.

[54] A.R. Khataee, G. Dehghan, E. Ebadi, and M. Pourhassan, *Central composite design optimization of biological dye removal in the presence of macroalgae chara sp*, CLEAN - Soil Air Water 38 (2010), pp. 750–757.

[55] A.R. Khataee and G. Dehghan, *Optimization of biological treatment of a dye solution by macroalgae Cladophora sp. using response surface methodology*, J. Taiwan. Inst. Chem. E 42 (2011), pp. 26–33.

[56] S. Sharma, A. Malik, and S. Satya, *Application of response surface methodology (RSM) for optimization of nutrient supplementation for Cr (VI) removal by Aspergillus lentulus AML05*, J. Hazard. Mater. 164 (2009), pp. 1198–1204.

[57] A. Aleboyeh, N. Daneshvar, and M.B. Kasiri, *Optimization of C.I. Acid Red 14 azo dye removal by electrocoagulation batch process with response surface methodology*, Chem. Eng. Process. 47 (2008), pp. 827–832.

[58] T. Ölmez, *The optimization of Cr(VI) reduction and removal by electrocoagulation using response surface methodology*, J. Hazard. Mater. 162 (2009), pp. 1371–1378.

[59] M. Zarei, A. Niaei, D. Salari, and A. Khataee, *Application of response surface methodology for optimization of peroxi-coagulation of textile dye solution using carbon nanotube-PTFE cathode*, J. Hazard. Mater. 173 (2010), pp. 544–551.

[60] L. Alidokht, A.R. Khataee, A. Reyhanitabar, and S. Oustan, *Reductive removal of Cr(VI) by starch-stabilized $Fe^0$ nanoparticles in aqueous solution*, Desalination 270 (2011), pp. 105–110.

[61] K.P. Singh, A.K. Singh, S. Gupta, and S. Sinha, *Optimization of Cr(VI) reduction by zero-valent bimetallic nanoparticles using the response surface modeling approach*, Desalination 270 (2011), pp. 275–284.

[62] A. Danion, C. Bordes, J. Disdier, J.-Y. Gauvrit, C. Guillard, P. Lantéri, and N. Jaffrezic-Renault, *Optimization of a single $TiO_2$-coated optical fiber reactor using experimental design*, J. Photochem. Photobiol., A 168 (2004), pp. 161–167.

[63] H.D. Mansilla, C. Bravo, R. Ferreyra, M.I. Litter, W.F. Jardim, C. Lizama, J. Freer, and J. Fernández, *Photocatalytic EDTA degradation on suspended and immobilized $TiO_2$*, J. Photochem. Photobiol., A 181 (2006), pp. 188–194.

[64] A.T. Hoke, *Economical second-order designs based on irregular fractions of the $3^n$ factorial*, Technometrics 16 (1974), pp. 375–384.

[65] M.J. Box and N.R. Draper, *Factorial designs, the $|X'X|$ criterion and some related matters*, Technometrics 13 (1971), pp. 731–742.

[66] K.G. Roquemore, *Hybrid designs for quadratic response surfaces*, Technometrics 18 (1976), pp. 419–423.

[67] M. Shen, Z. Wu, H. Huang, Y. Du, Z. Zou, and P. Yang, *Carbon-doped anatase $TiO_2$ obtained from TiC for photocatalysis under visible light irradiation*, Mater. Lett. 60 (2006), pp. 693–697.

[68] H.D. Mansilla, A. Mora, C. Pincheira, M.A. Mondaca, P.D. Marcato, N. Durán, and J. Freer, *New photocatalytic reactor with $TiO_2$ coating on sintered glass cylinders*, Appl. Catal., B 76 (2007), pp. 57–63.

[69] H. Yu, S.C. Lee, J. Yu, and C.H. Ao, *Photocatalytic activity of dispersed $TiO_2$ particles deposited on glass fibers*, J. Mol. Catal. A: Chem. 246 (2006), pp. 206–211.

[70] D. Robert, A. Piscopo, O. Heintz, and J.V. Weber, *Photocatalytic detoxification with $TiO_2$ supported on glass-fibre by using artificial and natural light*, Catal. Today 54 (1999), pp. 291–296.

[71] S. Horikoshi, N. Watanabe, H. Onishi, H. Hidaka, and N. Serpone, *Photodecomposition of a nonylphenol polyethoxylate surfactant in a cylindrical photoreactor with $TiO_2$ immobilized fiberglass cloth*, Appl. Catal., B 37 (2002), pp. 117–129.

[72] J.P. Boisvert, J. Peresello, A. Foissy, J.C. Castaing and B. Cabane, *Effect of surface charge on the adsorption mode of sodium poly(acrylate) on alumina-coated $TiO_2$ used as coating pigment*, Colloids Surf., A 168 (2000), pp. 287–296.

[73] R. Zallen and M.P. Moret, *The optical absorption edge of brookite $TiO_2$*, Solid State Commun. 137 (2006), pp. 154–157.

[74] A. Fujishima, T.N. Rao, and D.A. Tryk, *Titanium dioxide photocatalysis*, J. Photochem. Photobiol., C 1 (2000), pp. 1–21.

[75] M. Yao, J. Chen, C. Zhao, and Y. Chen, *Photocatalytic activities of Ion doped $TiO_2$ thin films when prepared on different substrates*, Thin Solid Films 517 (2009), pp. 5994–5999.

[76] V. Brezová, A. Blazková, L. Karpinský, J. Grosková, B. Havlínová, V. Jorík, and M. Ceppan, *Phenol decomposition using $M^{n+}/TiO_2$ photocatalysts supported by the sol-gel technique on glass fibres*, J. Photochem. Photobiol., A 109 (1997), pp. 177–183.

[77] E. Rego, J. Marto, P.S. Marcos, and J.A. Labrincha, *Decolouration of Orange II solutions by $TiO_2$ and ZnO active layers screen-printed on ceramic tiles under sunlight irradiation*, Appl. Catal., A 355 (2009), pp. 109–114.

[78] A. Rezaeea, M.T. Ghaneiana, N. Taghaviniab, M.K. Aminianb, and S.J. Hashemianc, *$TiO_2$ nanofibre assisted photocatalytic degradation of Reactive Blue 19 dye from aqueous solution* Environ. Technol. 30 (2009), pp. 233–239.

[79] A.M. Berto, *Ceramic tiles: above and beyond traditional applications*, J. Eur. Ceram. Soc. 27 (2007), pp. 1607–1613.

[80] K. Demeestere, J. Dewulf, B. De Witte, A. Beeldens, and H. Van Langenhove, *Heterogeneous photocatalytic removal of toluene from air on building materials enriched with $TiO_2$*, Build. Environ. 43 (2008), pp. 406–414.

[81] S. Zhang, N. Fujii, and Y. Nosaka, *The dispersion effect of $TiO_2$ loaded over ZSM-5 zeolite*, J. Mol. Catal. A: Chem. 129 (1998), pp. 219–224.

[82] J. Marto, P.S. Marcos, T. Trindade, and J.A. Labrincha, *Photocatalytic decolouration of Orange II by ZnO active layers screen-printed on ceramic tiles*, J. Hazard. Mater. 163 (2009), pp. 36–42.

[83] P.S. Marcos, J. Marto, T. Trindade, and J.A. Labrincha, *Screen-printing of $TiO_2$ photocatalytic layers on glazed ceramic tiles*, J. Photochem. Photobiol., A 197 (2008), pp. 125–131.

[84] G. Plesch, M. Gorbár, U.F. Vogt, K. Jesenák, and M. Vargová, *Reticulated macroporous ceramic foam supported $TiO_2$ for photocatalytic applications*, Mater. Lett. 63 (2009), pp. 461–463.

[85] Y. Xu and C.H. Langford, *Enhanced photoactivity of a titanium(IV) oxide supported on $ZSM_5$ and zeolite A at low coverage*, J. Phys. Chem-US 99 (1995), pp. 11501–11507.

[86] Y. Xu and C.H. Langford, *Photoactivity of titanium dioxide supported on MCM41, zeolite X and zeolite Y*, J. Phys. Chem-US 101 (1997), pp. 3115–3121.

[87] R.M. Mohamed, A.A. Ismail, I. Othman, and I.A. Ibrahim, *Preparation of $TiO_2$-ZSM-5 zeolite for photodegradation of EDTA*, J. Mol. Catal. A: Chem. 238 (2005), pp. 151–157.

[88] J. Villasenor, N. Duran, and H.D. Mansilla, *Photocatalyzed mineralization of kraft black liquor on $ZnO/Fe_2O_3$ coupled semiconductor*, Environ. Technol. 23 (2002), pp. 955–959.

[89] M. Anpo, M. Takeuchi, K. Ikeue, and S. Dohshi, *Design and development of titanium oxide photocatalysts operating under visible and UV light irradiation. The applications of metal ion–implantation techniques tosemiconducting $TiO_2$ and Ti/zeolite catalysts*, Curr. Opin. Solid State Mater. Sci. 6 (2002), pp. 381–388.

[90] H.R. Pouretedala, H. Beigyb, and M.H. Keshavarza, *Bleaching of Congo red in the presence of ZnS nanoparticles, with dopant of $Co^{2+}$ ion, as photocatalyst under UV and sunlight irradiations* Environ. Technol. 31 (2010), pp. 1183–1190.

[91] A.R. Khataee and M.B. Kasiri, *Photocatalytic degradation of organic dyes in the presence of nanostructured titanium dioxide: Influence of the chemical structure of dyes*, J. Mol. Catal. A: Chem. 328 (2010), pp. 8–26.

[92] V. Durgakumari, M. Subrahmanyam, K.V. Subba Rao, A. Ratnamala, M. Noorjahan, and K. Tanaka, *An easy and efficient use of $TiO_2$ supported HZSM-5 and $TiO_2$+HZSM-5 zeolite combinate in the photodegradation of aqueous phenol and p-chlorophenol*, Appl. Catal., A 234 (2002), pp. 155–165.

[93] C. Zhu, L. Wang, L. Kong, X. Yang, L. Wang, S. Zheng, F. Chen, F. MaiZhi, and H. Zong, *Photocatalytic degradation of AZO dyes by supported $TiO_2$ + UV in aqueous solution*, Chemosphere 41 (2000), pp. 303–309.

[94] M.V. Shankar, K.K. Cheralathan, B. Arabindoo, M. Palanichamy, and V. Murugesan, *Enhanced photocatalytic activity for the destruction of monocrotophos pesticide by $TiO_2/H$B*, J. Mol. Catal. A: Chem. 223 (2004), pp. 195–200.

[95] E.P. Reddy, L. Davydov, and P. Smirniotis, *$TiO_2$-loaded zeolites and mesoporous materials in the sonophotocatalytic decomposition of aqueous organic pollutants: the role of the support*, Appl. Catal., B 42 (2003), pp. 1–11.

[96] S. Fukahori, H. Ichiura, T. Kitaoka, and H. Tanaka, *Capturing of bisphenol a photodecomposition intermediates by composite $TiO_2$-zeolite sheets*, Appl. Catal., B 46 (2003), pp. 453–462.

[97] H. Yamashita, Y. Ichihashi, S.G. Zhang, Y. Matsumura, Y. Souma, T. Tatsumi, and M. Anpo, *Photocatalytic decomposition of NO at 275 K on titanium oxide catalysts anchored within zeolite cavities and framework*, Appl. Surf. Sci. 121–122 (1997), pp. 305–309.

[98] A.R. Khataee, M. Fathinia, S. Aber, and M. Zarei, *Optimization of photocatalytic treatment of dye solution on supported $TiO_2$ nanoparticles by central composite design: Intermediates identification*, J. Hazard. Mater. 181 (2010), pp. 886–897.

[99] A.R. Khataee, M. Zarei, and S.K. Asl, *Photocatalytic treatment of a dye solution using immobilized $TiO_2$ nanoparticles combined with photoelectro-Fenton process: optimization of operational parameters*, J. Electroanal. Chem. 648 (2010), pp. 143–150.

[100] A.R. Khataee, M. Zarei, M. Fathinia, and M.K. Jafari, *Photocatalytic degradation of an anthraquinone dye on immobilized $TiO_2$ nanoparticles in a rectangular reactor: destruction pathway and response surface approach*, Desalination 268 (2011), pp. 126–133.

[101] M. Fathinia, A.R. Khataee, M. Zarei, and S. Aber, *Comparative photocatalytic degradation of two dyes on immobilized $TiO_2$ nanoparticles: effect of dye molecular structure and response surface approach*, J. Mol. Catal. A: Chem. 333 (2010), pp. 73–84.

[102] I.H. Cho and K.D. Zoh, *Photocatalytic degradation of azo dye (Reactive Red 120) in $TiO_2/UV$ system: optimization and modeling using a response surface methodology (RSM) based on the central composite design*, Dyes Pigm. 75 (2007), pp. 533–543.

[103] J.M. Monteagudo and A. Durán, *Fresnel lens to concentrate solar energy for the photocatalytic decoloration and mineralization of orange II in aqueous solution*, Chemosphere 65 (2006), pp. 1242–1248.

[104] J. Fernández, J. Kiwi, J. Baeza, J. Freer, C. Lizama, and H.D. Mansilla, *Orange II photocatalysis on immobilised $TiO_2$: effect of the pH and $H_2O_2$*, Appl. Catal., B 48 (2004), pp. 205–211.

[105] M. Sleiman, D. Vildozo, C. Ferronato, and J.-M. Chovelon, *Photocatalytic degradation of azo dye Metanil Yellow: optimization and kinetic modeling using a chemometric approach*, Appl. Catal., B 77 (2007), pp. 1–11.

[106] H.L. Liu and Y.R. Chiou, *Optimal decolorization efficiency of Reactive Red 239 by $UV/TiO_2$ photocatalytic process*

*coupled with response surface methodology*, Chem. Eng. J. 112 (2005), pp. 173–179.

[107] M.S. Secula, G.D. Suditu, I. Poulios, C. Cojocaru, and I. Cretescu, *Response surface optimization of the photocatalytic decolorization of a simulated dyestuff effluent*, Chem. Eng. J. 141 (2008), pp. 18–26.

[108] A.L. Giraldo, G.A. Peñuela, R.A. Torres-Palma, N.J. Pino, R.A. Palominos, and H.D. Mansilla, *Degradation of the antibiotic oxolinic acid by photocatalysis with $TiO_2$ in suspension*, Water Res. 44 (2010), pp. 5158–5167.

[109] J. Zhang, D. Fu, Y. Xu, and C. Liu, *Optimization of parameters on photocatalytic degradation of chloramphenicol using $TiO_2$ as photocatalyist by response surface methodology*, J. Environ. Sci. 22 (2010), pp. 1281–1289.

[110] V.A. Sakkas, P. Calza, C. Medana, A.E. Villioti, C. Baiocchi, E. Pelizzetti, and T. Albanis, *Heterogeneous photocatalytic degradation of the pharmaceutical agent salbutamol in aqueous titanium dioxide suspensions*, Appl. Catal., B 77 (2007), pp. 135–144.

[111] J. Nieto, J. Freer, D. Contreras, R.J. Candal, E.E. Sileo, and H.D. Mansilla, *Photocatalyzed degradation of flumequine by doped $TiO_2$ and simulated solar light*, J. Hazard. Mater. 155 (2008), pp. 45–50.

[112] P. Calza, V.A. Sakkas, A. Villioti, C. Massolino, V. Boti, E. Pelizzetti, and T. Albanis, *Multivariate experimental design for the photocatalytic degradation of imipramine: determination of the reaction pathway and identification of intermediate products*, Appl. Catal., B 84 (2008), pp. 379–388.

[113] Y. Lin, C. Ferronato, N. Deng, F. Wu, and J.-M. Chovelon, *Photocatalytic degradation of methylparaben by $TiO_2$: Multivariable experimental design and mechanism*, Appl. Catal., B 88 (2009), pp. 32–41.

[114] V.A. Sakkas, P. Calza, M.A. Islam, C. Medana, C. Baiocchi, K. Panagiotou, and T. Albanis, *$TiO_2/H_2O_2$ mediated photocatalytic transformation of UV filter 4-methylbenzylidene camphor (4-MBC) in aqueous phase: Statistical optimization and photoproduct analysis*, Appl. Catal., B 90 (2009), pp. 526–534.

[115] S.A.V. Eremia, D. Chevalier-Lucia, G.-L. Radu, and J.-L. Marty, *Optimization of hydroxyl radical formation using $TiO_2$ as photocatalyst by response surface methodology*, Talanta 77 (2008), pp. 858–862.

[116] S. Ray, J.A. Lalman, and N. Biswas, *Using the Box-Benkhen technique to statistically model phenol photocatalytic degradation by titanium dioxide nanoparticles*, Chem. Eng. J. 150 (2009), pp. 15–24.

[117] S.K. Kansal, M. Singh, and D. Sud, *Parametric optimization of photocatalytic degradation of catechol in aqueous solutions by response surface methodology*, Indian J. Chem. Technol. 14 (2007), pp. 145–153.

[118] R.H. Myers and D.C. Montgomery, *Response Surface Methodology, Process and Product Optimization using Designed Experiments*, John Wiley & Sons, Inc., New York 2002.

[119] X. Zhang, R. Wang, X. Yang, and J. Yu, *Central composite experimental design applied to the catalytic aromatization of isophorone to 3,5-xylenol* Chemom. Intell. Lab. Syst. 89 (2007), pp. 45–50.